Design of Machines and Structures, Vol. 11, No. 2 (2021), pp. 36–43.
https://doi.org/10.32972/dms.2021.013
http://orcid.org/0000-0002-9636-827 *(Sz. Nagy)*
http://orcid.org/0000-0001-8487-4327 *(K. Jármai)*
http://orcod.org/0000-0003-2727-2498 *(A. Baksa)*

EVOLUTIONARY OPTIMIZATION OF A TRANSMISSION LINE TOWER WITH FPA ALGORITHM

SZILÁRD NAGY[1] – KÁROLY JÁRMAI[2] – ATTILA BAKSA[3]

University of Miskolc,
[1,2]Institute of Energy Engineering and Chemical Machinery,
[3]Institute of Applied Mechanics
3515 Miskolc-Egyetemváros, Hungary
szilard.nagy@emerson.com, karoly.jarmai@uni-miskolc.hu,
attila.baksa@uni-miskolc.hu

Abstract: The optimization of the pylon is shown in this paper. The optimization is made by using flower pollination algorithm. The objective function is mass of the structure. The design constraints are static stress, local buckling and buckling. The unknowns are the typical dimensions of the circular hollow section truss. Parametric inspections have been made changing yield strength of material and the number of grid divisions. The results show that the use of higher yield strength steels, do not imply a lighter structure.

Keywords: *evolutionary optimization, finite element method, pylon, truss structure*

1. INTRODUCTION

Metaheuristic and nature inspired evolutionary algorithms are efficiently used for solving non-linear engineering problems, such as many dimensional optimization problems. Xin-She Yang proposed the flower pollination [4]. It is inspired by the reproduction process of plants. The Flower pollination algorithm like most evolutionary algorithms is developed for solving continuous, unconstrained optimization problems.

Usually transmission line towers, pylons are made from angle section trusses [1], [2]. The buckling stiffness of angle sections are very small. Orbán et al. [3] had shown the usage of a circular hollow section (CHS) is more favorable.

In this paper, we inspect whether the use of higher yield strength steel has additional beneficial effects for CHS.

2. FLOWER POLLINATION ALGORITHM [FPA]

Flower pollination is a major reproduction process of plants. It can take two forms, abiotic (local) and biotic (global). Pollens are transferred long distances during global pollination by pollinators such as insects, birds, wind, etc. This is specific to about 90% of flowering plants. The Abiotic form does not require any pollinator. This inspired a method to develop FPA algorithm in [4].

In the FPA algorithm, global pollination is modelled by following equation

$$^{(G+1)}\mathbf{x}_{Gi} = {}^{(G)}\mathbf{x}_i + L\left({}^{(G)}\mathbf{x}_i - {}^{(G)}\mathbf{g}_*\right) \tag{1}$$

where (G) is G^{th} generation, $\mathbf{x}_i$ is i^{th} individual in population, L is a Levy distribution random number and $\mathbf{g}_*$ represents the fittest individual in a population. Local pollination can be described

$$^{(G+1)}\mathbf{x}_{Li} = {}^{(G)}\mathbf{x}_i + \epsilon\left({}^{(G)}\mathbf{x}_j - {}^{(G)}\mathbf{x}_k\right) \quad i \neq j \neq k \tag{2}$$

where ϵ is a uniform distribution random number in $[0,1]$ interval and j, k are random indicies. A p probability variable decides between the two mutation methods. A more detailed description and complete algorithm can be found in [4]

$$^{(G+1)}\mathbf{x}_i = \begin{cases} ^{(G+1)}\mathbf{x}_{Gi} & p \leq \text{rand}[0,1) \\ ^{(G+1)}\mathbf{x}_{Li} & \text{otherwise} \end{cases} \tag{3}$$

3. INSPECTED PYLON WITH THEIR LOADS

In the present case, the subject of the investigation is a 45 m high intermediate pylon. The structure can be divided into two parts, a 21 m high top and a 24 m high bottom. The loads were according to [5]. The size-giving load is half a wire pull. Without detailing the calculations from [1] forces transmitted from the upper pylon part are $F_V = 209.03$ kN vertical force, $F_H = 312.14$ kN horizontal force and $M_h = 2850.5$ kNm bending moment. In the load calculations 400 m span length, weight of 12 pieces wire and 1.1 safety factor are applied.

Forces reduced to vertices as shown in

$$F_{y1} = \frac{M_h}{2a_2} - \frac{F_v}{4} = \frac{2850.5 \text{ kNm}}{2 \cdot 3.7 \text{ m}} - \frac{209.03 \text{ kN}}{4} = 332.94 \text{ kN} \tag{4}$$

$$F_{y2} = \frac{M_h}{2a_2} + \frac{F_v}{4} = \frac{2850.5 \text{ kNm}}{2 \cdot 3.7 \text{ m}} + \frac{209.03 \text{ kN}}{4} = 437.46 \text{ kN} \tag{5}$$

where $a_2 = 3{,}7\ m$ is the width of the upper pylon part. It is sufficient to perform the calculations on only one inclined plane relevant to the loads as shown on . In the case of a pyramid with a side skew of $\beta = 80°$, the forces acting on the inclined plane under investigation, as indicated in

$$F_1 = \frac{F_{y1}}{\sin\beta} = \frac{332.94 \text{ kN}}{\sin 80°} = 338.08 \text{ kN} \tag{6}$$

$$F_2 = \frac{F_{y2}}{\sin \beta} = \frac{437.46\ \mathrm{kN}}{\sin 80°} = 444.21\ \mathrm{kN} \tag{7}$$

$$F_3 = \frac{F_h}{2} = \frac{312.14\ \mathrm{kN}}{2} = 338.08\ \mathrm{kN} \tag{8}$$

illustrates an example with a grid of $n_g = 2$. During further investigations, several grid division tasks will be solved. Grid divisions are reduced or increased based on the following relationship

$$h_1 = \frac{h}{2.5 n_g} \tag{9}$$

Trusses of the planar truss model were classified into three cross-sectional groups. The first group consists of the elements of the side column (1–10 trusses). Members of the second group are horizontal elements (17–22 trusses). Finally, the third group consists of grid elements forming a deltoid and a triangle (23–26 trusses). In each cross-section group, the circular section is used, the characteristic dimensions of which are shown in *Figure 3*

Cross-section of circular tube. Such as outer diameters D_1, D_2, D_3 and wall thicknesses t_1, t_2, t_3.

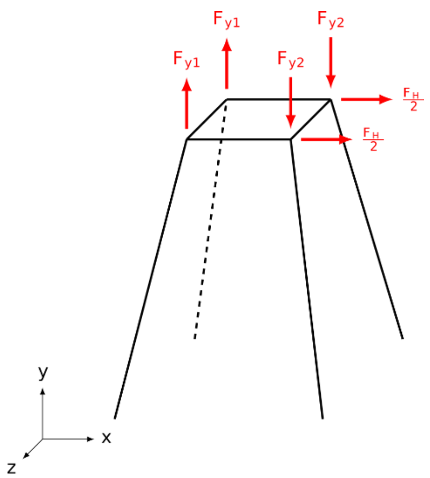

Figure 1
Sketch of lower part of pylon

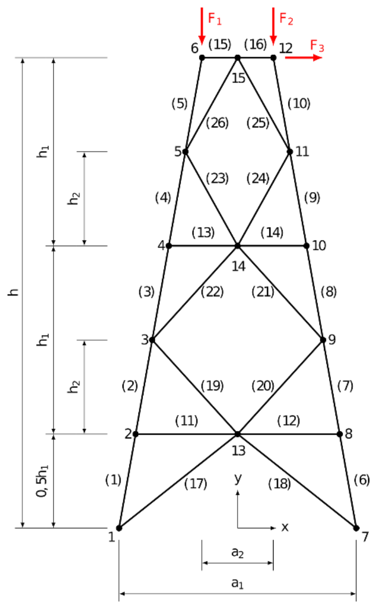

Figure 2
Planar truss structure

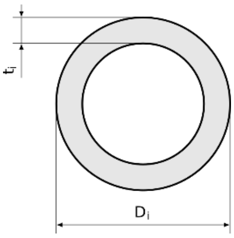

Figure 3

Cross-section of circular tube

4. APPLIED FINITE ELEMENT MODEL

In this case the planar structure could be modelled as a pushed and pulled truss model, as shown in *Figure 4*.

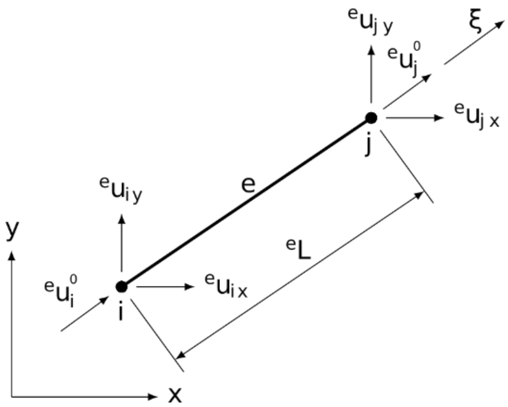

Figure 4

Finite element model of truss

Node displacement is only possible along the ξ axis (local coordinate system) passing through nodes i and j. In the *x*-*y* global coordinate system, the *x*, *y* projections of this displacement are interpreted

$$ {}^{e}\mathbf{u}' = \left[{}^{e}u_i' \quad {}^{e}u_j' \right]^T \qquad {}^{e}\mathbf{u} = \left[{}^{e}u_{ix} \quad {}^{e}u_{iy} \quad {}^{e}u_{jx} \quad {}^{e}u_{jy} \right]^T \tag{10} $$

The transition between the two coordinate systems is possible with the transformation matrix

$$ {}^{e}T = \begin{bmatrix} {}^{e}T_{11} & {}^{e}T_{12} & 0 & 0 \\ 0 & 0 & {}^{e}T_{23} & {}^{e}T_{24} \end{bmatrix} \tag{11} $$

$$ {}^{e}T_{11} = {}^{e}T_{23} = \frac{{}^{e}u_{jx} - {}^{e}u_{ix}}{{}^{e}L} \qquad {}^{e}T_{12} = {}^{e}T_{24} = \frac{{}^{e}u_{jy} - {}^{e}u_{ix}}{{}^{e}L} \tag{12} $$

In equilibrium, the total Π potential energy is minimal, that is mean the $\delta\Pi$ first variation of potential energy is zero for whole structure. The total potential energy for elements is depicted in the local and then global coordinate system

$$ {}^{e}\Pi' = \frac{1}{2} \cdot {}^{e}\mathbf{u}'^{T} \cdot ({}^{e}\mathbf{K}' \cdot {}^{e}\mathbf{u}' - {}^{e}\mathbf{f}') \tag{13} $$

$$ {}^{e}\Pi = \frac{1}{2} \cdot {}^{e}\mathbf{u}^{T} \cdot ({}^{e}\mathbf{K} \cdot {}^{e}\mathbf{u} - {}^{e}\mathbf{f}) \tag{14} $$

where $\mathbf{f}$ is a generalized loads vector reduced to nodes, and $\mathbf{K}'$, $\mathbf{K}$ are the stiffness matrices in local and global coordinate systems

$$ {}^{e}\mathbf{K}' = \frac{{}^{e}E \cdot {}^{e}A}{{}^{e}L} \begin{bmatrix} 1 & -1 \\ -1 & 1 \end{bmatrix} \tag{15} $$

$$ {}^{e}\mathbf{K} = {}^{e}\mathbf{T}^{T} \cdot {}^{e}\mathbf{K}' \cdot {}^{e}\mathbf{T} \tag{16} $$

Introducing $\mathbf{u}$ vector of nodal displacements and $\mathbf{f}$ load vectors of the total system potential energy

$$ \mathbf{u} = [{}^{1}\mathbf{u} \quad {}^{2}\mathbf{u} \quad {}^{3}\mathbf{u} \quad \cdots \quad {}^{e}\mathbf{u}]^{T} \qquad \mathbf{f} = [{}^{1}\mathbf{f} \quad {}^{2}\mathbf{f} \quad {}^{3}\mathbf{f} \quad \cdots \quad {}^{e}\mathbf{f}]^{T} \tag{17} $$

$$ \delta\Pi = 0 = \frac{1}{2}\delta\mathbf{u}^{T}(\mathbf{K}\mathbf{u} - \mathbf{f}) \tag{18} $$

where $\mathbf{K}$ is the stiffness matrix of the whole system, the elements of this must be determined according to the rules of element fitting [6]–[8]. Also, the boundary conditions should be applied to (18) equation. A non-trivial solution of (18) exists only if the term in parentheses is zero.

Stress of elements could be calculated from the nodal displacement vector

$$ {}^{e}\sigma = \frac{{}^{e}E}{{}^{e}L} \cdot [-{}^{e}T_{11} \quad -{}^{e}T_{12} \quad {}^{e}T_{11} \quad {}^{e}T_{12}] \cdot {}^{e}\mathbf{u} \tag{19} $$

5. THE OPTIMIZATION PROBLEM

During the optimization, the minimal mass of the structure was searched

$$ \min\left(\sum_{i=1}^{n_e} m_i\right) = \min\left(\rho \sum_{i=1}^{n_e} A_i L_i\right) \tag{20} $$

where m_i is the mass of elements, $\mathrm{A_i}$ is the cross-sectional area of elements, L_i is length of elements and ρ is the density of elements. This optimization is a constrained optimization because the structure must meet strength and stability requirements. In the present case, three criteria have been considered, such as resistance to tensile, buckling, and local buckling. These constraints can be well characterized by the cross-sectional utilization factors.

The first constraint of each element contains the resistance to tensile and buckling

$$\mathrm{g_{Ii}} = \begin{cases} \dfrac{\gamma_{M0}|{}^{e}\sigma|}{\chi f_y} & {}^{e}\sigma < 0 \\ \dfrac{\gamma_{M0}|{}^{e}\sigma|}{f_y} & {}^{e}\sigma \geq 0 \end{cases} \tag{21}$$

where f_y is the yield strength, γ_{M0} is the generalized safety factor according to [9], and χ is the buckling factor according to [9]. If the stress is less than zero, that means the load is pushing, otherwise the load is pulling. Second constraints of each element come from criteria of local buckling. Recommendations of [9] for diameter and wall thickness ratio of circular hollow section

$$\mathrm{g_{IIi}} = \frac{D_i f_y}{21150 t_i} \tag{22}$$

Equation (22)(22) is true only if the unit of f_y yield strength is MPa, and the unit of D_i, t_i dimensions are mm. The value of $\mathrm{g_{Ii}}$ must be calculated for each truss, while $\mathrm{g_{IIi}}$ is sufficient only once for each cross-sectional group.

According to previously described equations the fitness function of optimization

$$\mathcal{F}(D_1, D_2, D_3, t_1, t_2, t_3) = \sum_{i=1}^{n_e} m_i + \sum_{i=1}^{n_e} p_{Ii} + \sum_{i=1}^{3} p_{IIi} \tag{23}$$

where $\mathrm{p_{Ii}}$ and $\mathrm{p_{IIi}}$ are the "death" penalty functions

$$\mathrm{p_{Ii}} = \begin{cases} 0 & \mathrm{g_{Ii}} \leq 1 \\ 10^6 \mathrm{g_{Ii}} & \mathrm{g_{Ii}} > 1 \end{cases} \tag{24}$$

$$\mathrm{p_{Ii}} = \begin{cases} 0 & \mathrm{g_{Ii}} \leq 1 \\ 10^6 \mathrm{g_{IIi}} & \mathrm{g_{IIi}} > 1 \end{cases} \tag{25}$$

6. RESULTS OF OPTIMIZATION

During the optimization, more grid divisions $n_g = 1 \cdots 6$ are investigated, with different base materials. The yield strength of the inspected structural steels varied

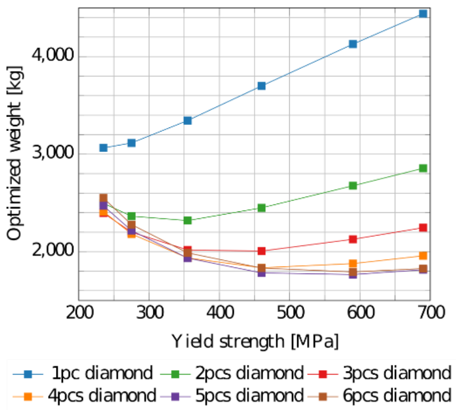

Figure 5
Optimized weight

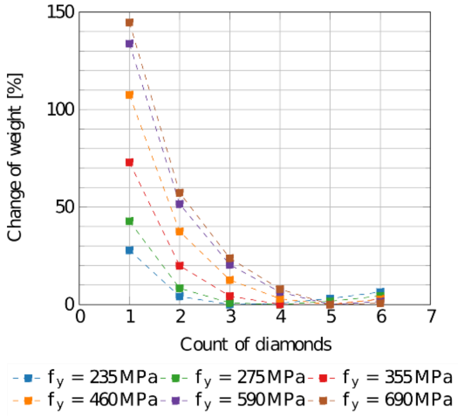

Figure 6
Percentage change in optimized weight

between 235 MPa and 690 MPa. During running of optimization, the fitness function was converging continuously to a minimum value.

Results of optimization shown in *Figure 5* and *Figure 6*. As can be seen, the use of higher yield strength steel does not clearly result in a lighter structure. The number of grid divisions should also increase to achieve less weight. An increase in yield strength on one side improves the overall resistance of the element, but on the other hand worsens the buckling factor. The optimal result is obtained when these two effects are balanced. In this case the optimal result is when yield strength is $f_y = 460$ MPa and number of grid divisions is $n_g = 5$.

7. Conclusions

The combination of flower pollination algorithm and finite element method is efficiently used for optimizing truss like structures. In this case optimizing the lower part of a pylon. The iterative calculation process is easy to automate and does not require derivatives that are difficult to produce. The presented method can be easily adopted to solve other truss problems as well.

The results of optimization show that, usage of higher strength steel dose not contribute to a lighter structure without changing the topology.

Acknowledgement

The research was supported by the Hungarian National Research, Development and Innovation Office—NKFIH under the project number K 134358.

REFERENCES

[1] Rao, G. V. (1995). Optimum design for transmission line towers. *Computers & Structures*, Vol. 57, No. 1, pp. 81–92.

[2] Silva, J. G. S., Vellasco, P. C. G., Andrade, S. A. L., Oliveira, M. I. R. (2005). Structural steel design and behaviour; Steel structures; Spatial structures; Telecommunication and transmission towers. *Journal of Constructional Steel Research*, Vol. 61, No. 8.

[3] Orbán, F., Farkas, J., Jármai, K. (2011). Optimum design of a transmission line tower : Welded tubular truss structure. *6th European Conference on Steel and Composite Structures*, Eurosteel 2011, Brussels.

[4] Yang, X. S. (2012). *Flower pollination algorithm for global optimization, Unconventional Computation and Natural Computation*. Springer Berlin Heidelberg, Berlin.

[5] MSZ 151-1:2000 (2000). *Power overhead lines. Installation requirements for overhead lines with a nominal voltage greater than 1 kV*. Magyar Szabványügyi Testület, Budapest (in Hungarian).

[6] Páczelt, I. (1999). *Finite element method in engineering practice*. Miskolci Egyetemi Kiadó, Miskolc (in Hungarian).

[7] Ferreira, A. J. M. (2009). MATLAB Codes for Finite Element Analysis. Springer Netherlands, Amsterdam.

[8] Smith M. I.; Lee M.; Programming the Finite Element Method, 4th edition, ISBN 0-470-84969-3, John Wiley and Sons Ltd, London, 2004

[9] EN 1993-1-1:2009; Eurocode 3: Design of steel structures - part 1-1: General rules and rules for buildings, European Committee Standardization, Brussels, 2009.